International Journal of Pure and Applied Physics
ISSN 0973-1776 Volume 3 Number 1 (2007) pp. 49–58

http://www.ripublication.com/ijpap.htm

Optical Properties of $Bi_{30}Se_{(70-x)}Te_x$ Amorphous Thin Films

A.S. Abd-Rabo and K.A. Sharaf

Physics Department, Faculty of Science,
Al-Azhar University for Girl's, Nasr City, Cairo, Egypt

Abstract

The optical properties of vacuum deposited $Bi_{30}Se_{(70-x)}Te_x$ amorphous thin films (where x = 35, 40 and 45 at%) with different thicknesses (150,200,250 nm) were studied in the wavelength range (400-900 nm). It was found that the optical absorption is due to indirect transition and the energy gap decreases with increasing Te content. The optical band gap Eg was found to be almost thicknesses independent. The optical constants n, k the real and imaginary parts of the dielectric constant have been also calculated.

Introduction

The amorphous semiconductors, especially chalcogenide glasses have received a great deal of attention because of their importance in some technological applications, such as elecrophotography, videos, photocells, rectifiers, infrared transmitting window, electrical and optical memory and more recently the electronic switching. These glasses are easily formed by melt quenching over a large range of composition making them suitable model systems for the investigation of composition dependence of their properties, such dependence for optical [1-5] and electrical [6,7] properties were recently reported. In the present article the optical properties of Bi_{30} $Se_{(70-x)}$ Te_x amorphous thin films where (x=35, 40 and 45 at %) have been studied, where the prepared films have thicknesses (150,200, and 250 nm)

Experimental Techniques

Samples under investigation were prepared from highly pure Bi, Te and Se (99,999%) purity, supplied by Aldrich Chemical Company (USA). The constituents were weighted in accordance with their atomic percentages. Pure elements were placed into a silica tube. The contents of the tube were sealed in a vacuum of 10^{-4} torr and heated in a furnace at about 1000°C for 15h and shaken several times during the course of heating to ensure a high degree of homogeneity. The melt was quenched in ice water to obtain the glass. X-ray diffractometry using Cu K_α as an incident radiation, proved the amorphous nature of the formed composition.

Thin film samples having thickness of 150, 200 and 250 nm were prepared by thermal evaporation technique onto thoroughly cleaned glass substrates using Edward 306 E Coating unit. A vacuum of the order of 10^{-6} torr was maintained during the vaporization process. The thickness of films was determined by a thickness monitor. X-ray diffraction investigations were carried out to identify the structure of the prepared films. All prepared films exhibit amorphous structure. The reflection and transmission of the prepared films were measured in the spectral range 190-2500 nm using the Jasco V-570 spectrophotometer.

Results and Discussion

Fig. (1) shows the X-ray diffraction data of the prepared films. No diffraction peaks are observed indicating the amorphous nature of all films.

For the determination of the optical band gap , E_g , the procedure suggested by De Michelis [8] was used near the absorption edge. The reflectance R and T transmittance are related to the absorption coefficient α by

$$T = (1-R)\exp(-\alpha d) \qquad (1)$$

where d is the thickness of the film, then

$$\alpha = 1/d \ln[(1-R)/T] \qquad (2)$$

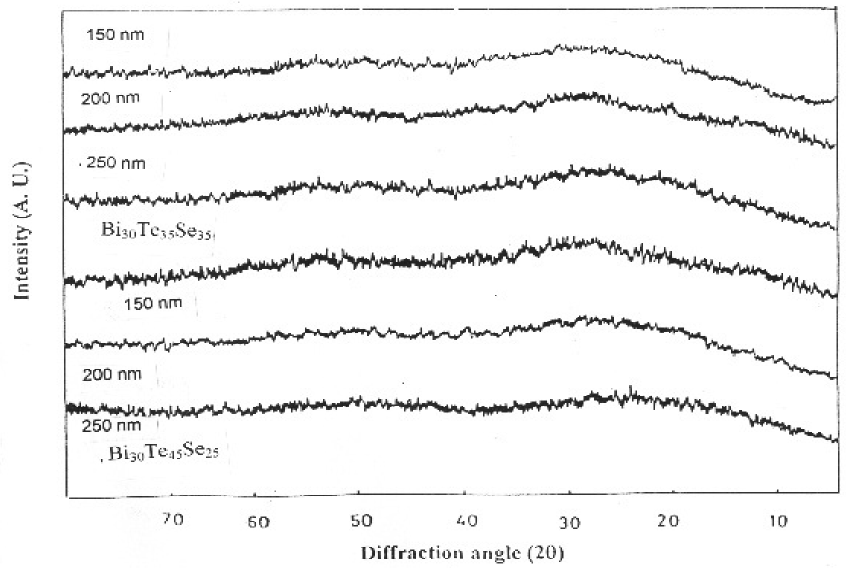

Figure 1: X-ray diffraction patterns for $Bi_{30}Te_{35}Se_{35}$, and $Bi_{30}Te_{45}Se_{25}$ with thickness (150,200,250 nm).

By measuring R and T at different wavelengths, α can be estimated. The spectral dependence of the absorption coefficient has the form

$\alpha\hbar w = \beta (\hbar w - E_g)^n$ (3)

where E_g is the optical gap, β is the edge width parameter and n is an integer equal 1,2 or 3 the value of n depends on the types of transition (direct or indirect) and the structure features of the film (crystalline or amorphous). The plots in Figs. (2-a,b) fit the linear relation $(\alpha\hbar w)^{1/2}$ versus ħω for all thicknesses. Values of E_g and β^{-1} are given in table (1).

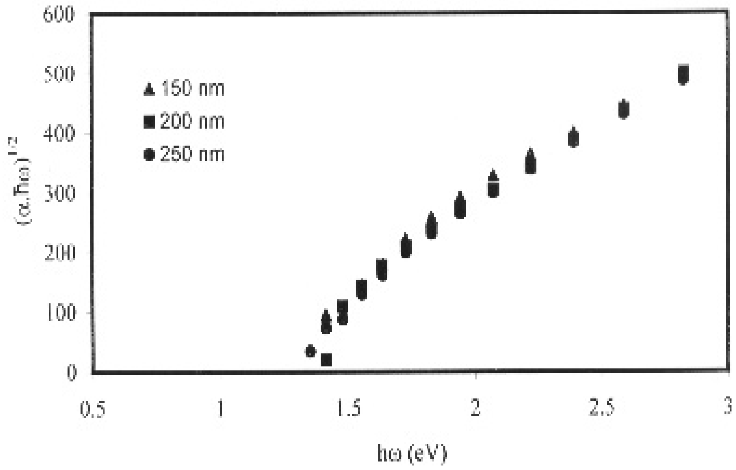

Figure (2-a): Relation between the $(\alpha.\hbar\omega)^{1/2}$ and ħω for $Bi_{30} Te_{35} Se_{35}$

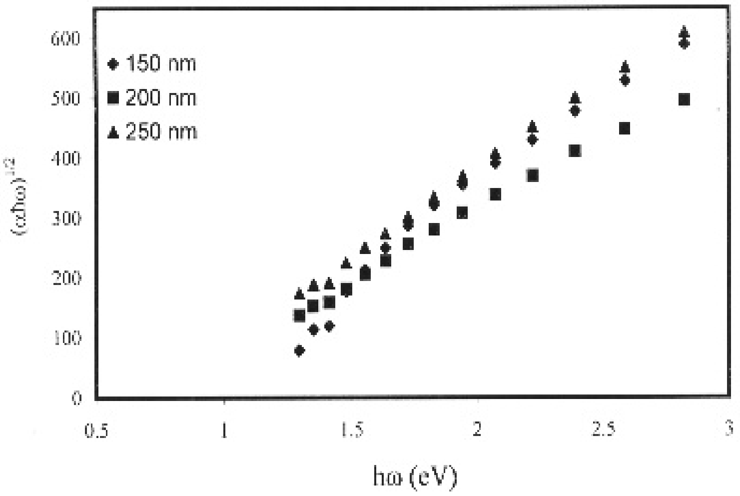

Figure (2-b): Relation between the $(\alpha.\hbar\omega)^{1/2}$ and ħω for $Bi_{30} Te_{45} Se_{25}$

The width of the band tail is shown also in Table (1). The values were calculated using Urbach's empirical relation:

$\ln \alpha = \ln A - (\hbar\omega / E_t)$ (4)

where A is a constant and E_t is the width of the band tails of the localized states in the band gap.

It should be mentioned that equation (4) is applicable only in the low absorption region ($\alpha = 10^3$–10^4 cm^{-1}) Figs. (3-a,b) represent the linear dependence of ln α on the photon energy ħω for all investigated films. The slope of each line yields the magnitude of E_t. The measured values of E_t as a function of thickness are recorded in Table (1).

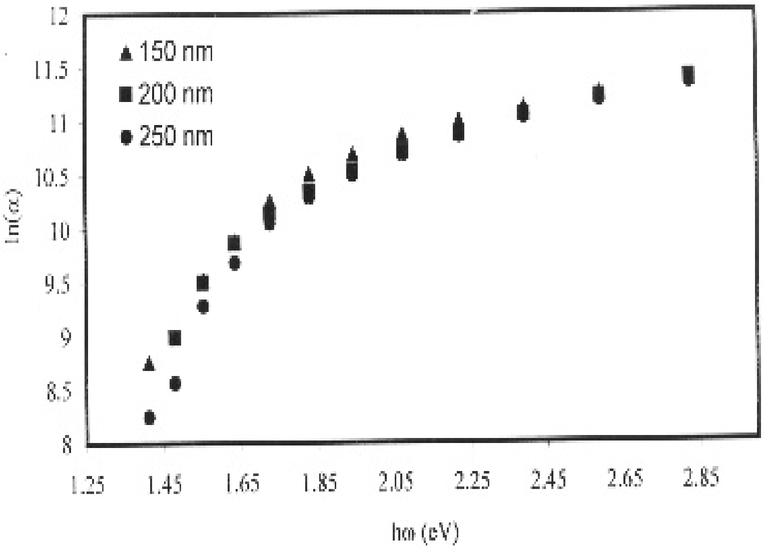

Figure (3-a): Relation between the In (α) and hω (ev) for Bi_{30} Te_{35} Se_{35}

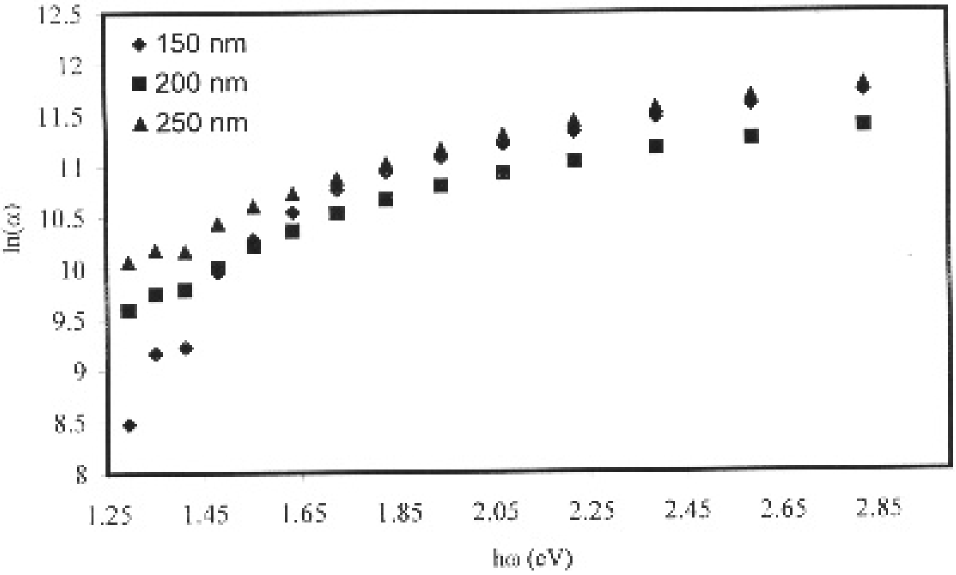

Figure (3-b): Relation between the In (α) and hω (ev) for Bi_{30} Te_{45} Se_{25}

The table shows that the energy gap decreases with increasing Te content and almost thicknesses independent. The decrease in the energy gap may be explained by recalling Kastner [10] suggestion that, the lon pair (Lp) electrons adjacent to electro positive atoms will have higher energies than those close to electronegative atoms. Therefore, addition of higher electropositive elements to the alloys, may raise the energy of some Lp states and consequently to broaden further the band to the forbidden gap for selenium element, the electronegativities are 2.4 and 2.1 for Se and Te, respectively. Hence, substitution of Te (less electronegative) for Se in these samples would expect to raise, some of the Lp states and broaden the and broaden the valence band, giving rise to additional absorption over wider energy range.

Table 1: the values E_g , β^{-1} and E_t for all samples

Composition	**Thickness (nm)**	**E_g (ev)**	**β^{-1} (ev cm)**	**E_t (ev)**
Bi_{30} Te_{35} Se_{35}	150	0.92	1.35×10^{-5}	0.25
	200	0.94	1.38×10^{-5}	0.30
	250	0.95	1.42×10^{-5}	0.32
Bi_{30} Te_{40} Se_{30} [9]	150	0.76	5.6×10^{-6}	0.58
	200	0.72	7.8×10^{-6}	0.60
	250	0.68	6.76×10^{-6}	0.62
Bi_{30} Te_{45} Se_{25}	150	0.60	1.29×10^{-5}	0.2
	200	0.62	1.33×10^{-5}	0.18
	250	0.63	1.32×10^{-5}	0.17

The optical constants of the investigated films were calculated using the following equation [11]

$$K = \frac{\alpha\lambda}{4\pi} \quad , \qquad n = \left(\frac{\left(1 + \sqrt{R}\right)}{\left(1 - \sqrt{R}\right)} \right) \tag{5}$$

where K is the extinction coefficient, λ is the wavelength of the radiation in vacuum, n is the refractive index and R is the reflection coefficient.

The optical constants were calculated from the eq. (5) and the values of the optical constants n and K for $Bi_{30}Te_{35}Se_{35}$ and $Bi_{30}Te_{45}Se_{25}$ are plotted as a function of wavelength of different thicknesses, through the investigated range of spectra (400-900 nm) in Figs. (4-5). It is clear from these figures, that the reflective index (n) increases, (K) decreases with the increase of wavelength. The samples have high values of refractive index, which are useful in the industry of reflectors.

The real and imaginary parts of dielectric constant can be calculated by using equation (6) where

$$\varepsilon' = n^2 - K^2 = 2nK \tag{6}$$

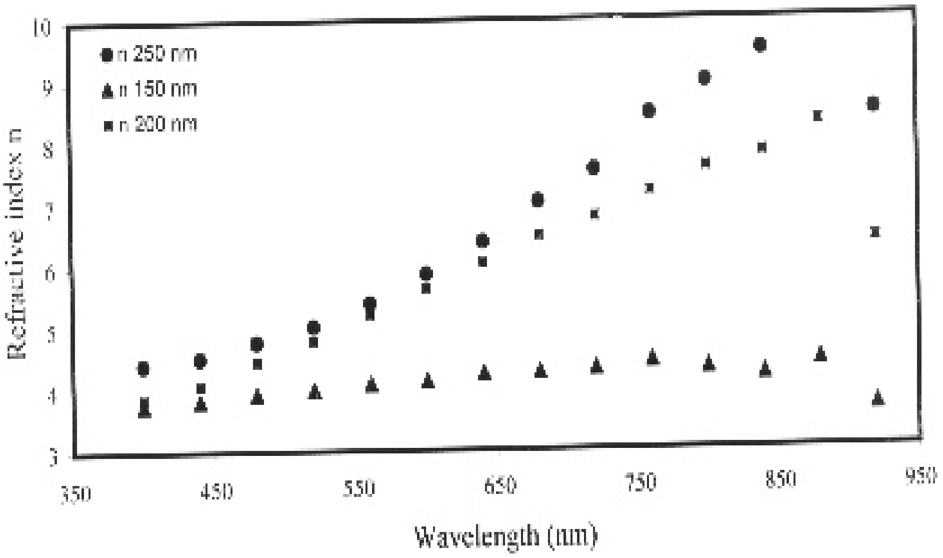

Figure (4-a): Relation between the refractive index and the wavelength for Bi_{30} Te_{35} Se_{35}

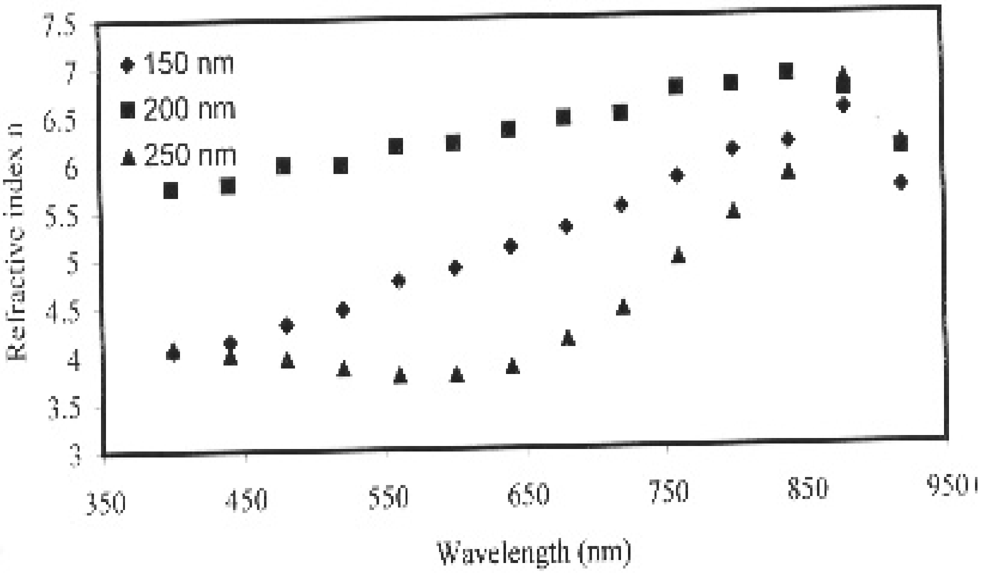

Figure (4-b): Relation between the refractive index and the wavelength for Bi_{30} Te_{45} Se_{25}.

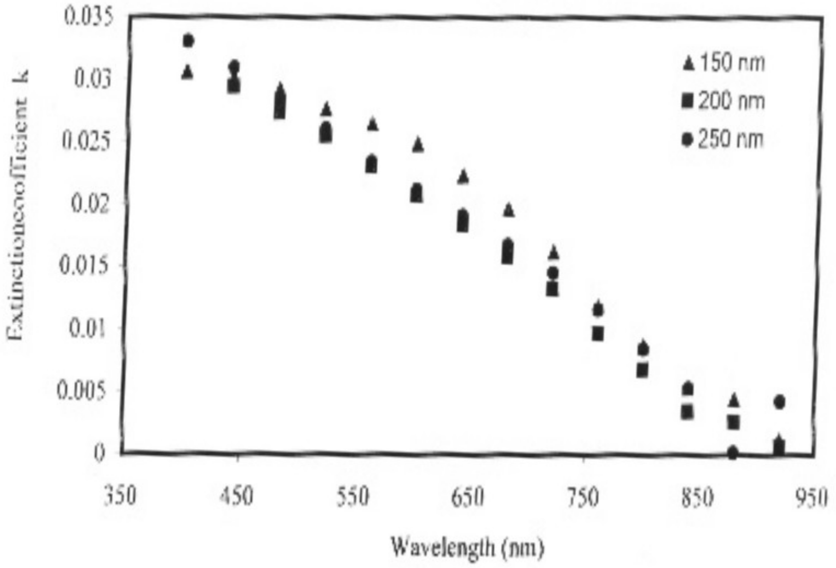

Figure (5-a): Relation between the extinction coefficient and the wavelength for Bi_{30} Te_{35} Se_{35}

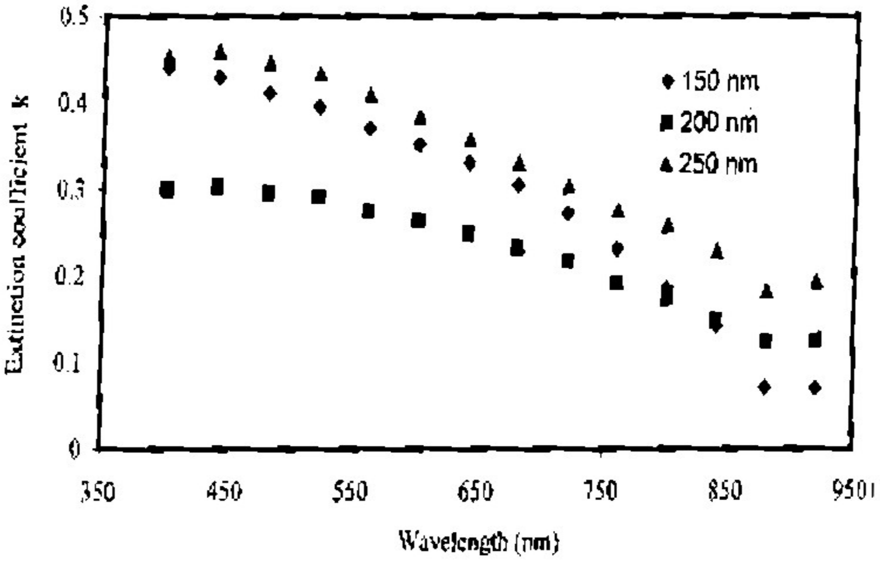

Figure (5-b): Relation between the extinction coefficient and the wavelength for Bi_{30} Te_{45} Se_{25}

Figures (6 and 7) show the dielectric constant ε', ε" versus the photon energy for the samples.

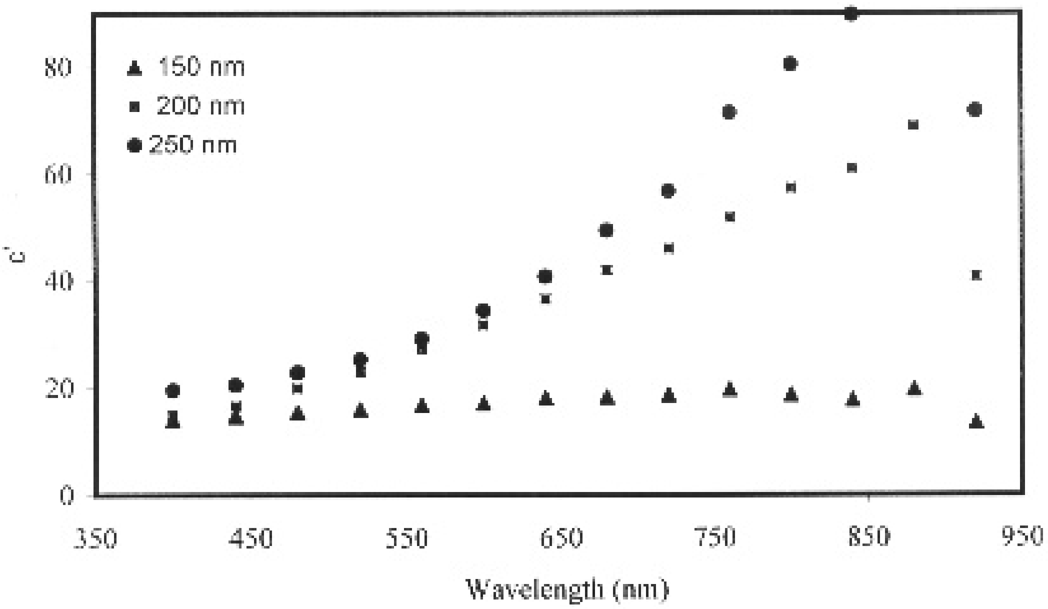

Figure (6-a): Relation between the real part of dielectric constant and the wavelength for $Bi_{30}Te_{35}Se_{35}$

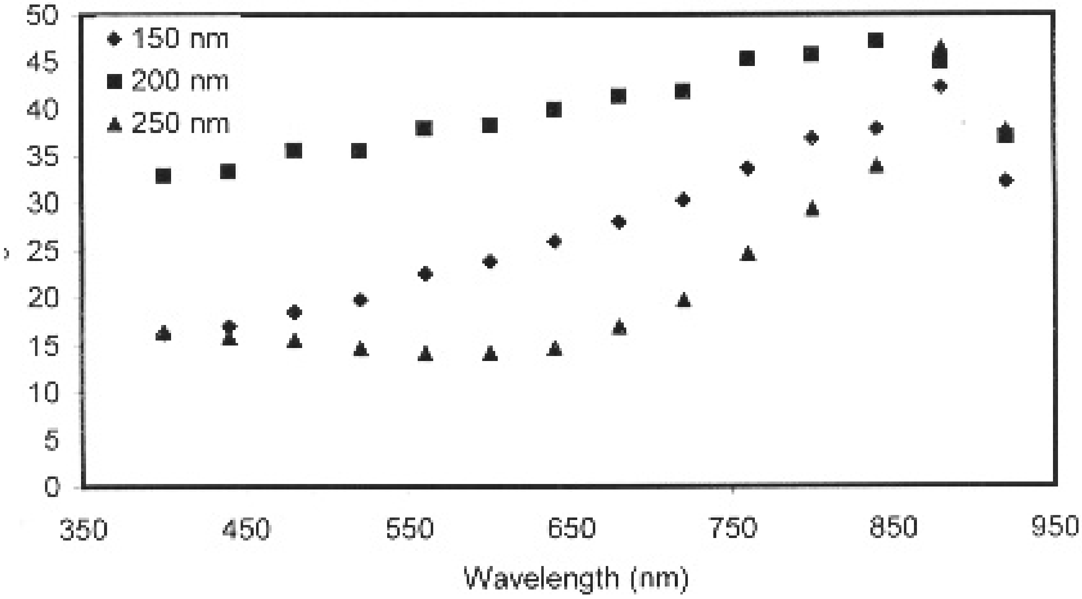

Figure (6-b): Relation between the real part of dielectric constant and the wavelength for $Bi_{30}Te_{45}Se_{25}$

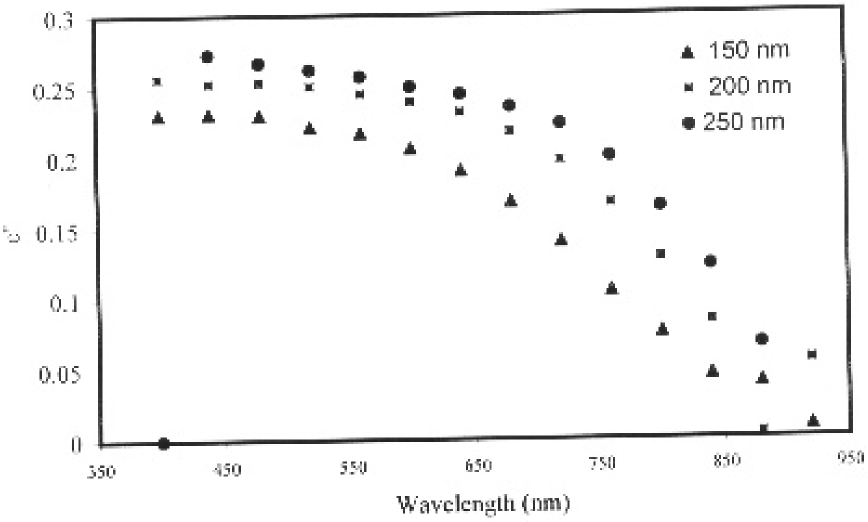

Figure (7-a): Relation between the imaginary part of dielectric constant and the wavelength for $Bi_{30}Te_{35}Se_{35}$.

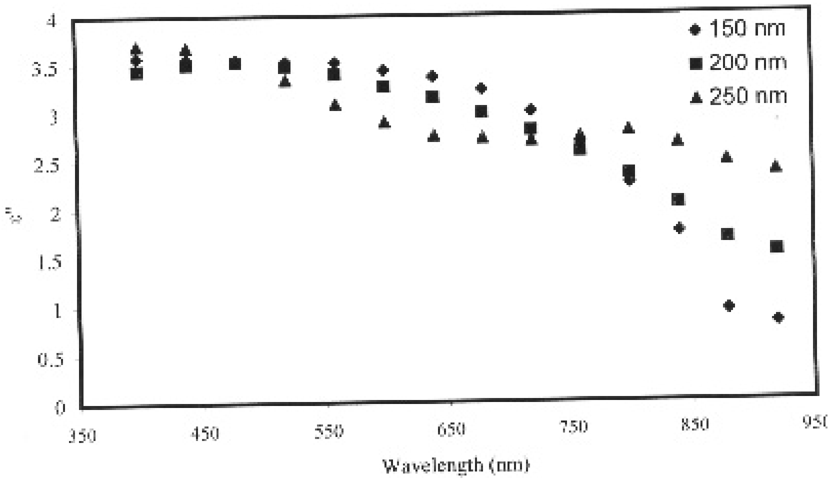

Figure (7-b): Relation between the imaginary part of dielectric constant and the wavelength for $Bi_{30}Te_{45}Se_{25}$

Conclusions

The optical properties of $Bi_{30}Se_{(70-x)}Te_x$ amorphous thin films were investigated at room temperature. The band tail width obeys Urbach's empirical relation. The optical absorption is due to indirect transition and the energy gap decreases with increasing Te content. The optical band gap E_g was found to be almost thickness independent. The value of the index of refraction n is higher than the extinction k through the investigated range.

References

[1] V. Pamu Kchieva, A. Szekeres, E. Savova, E. Vlaikova, J. Non-cryst. Solids 242 (1998) 110.

[2] E. Marquez, P. Nagels, J.M. Gonzalez-leal, A.M. Bernal Oliva, E. Sleecky. R. Callaerts, Vacuum 52 (1999) 55.

[3] Kazuhiko Ogusu, Shinpei Maeda, Michihiko Kitao, Honpuli, Makoto Minakoto, J. Non-cryst. Solids 347 (2004) 159-165.

[4] N-Tohge, T. Minami, Y.Yamamoto and M. Tanaka, J. Appl.Phys. 51 (1980) 1048.

[5] N. Tohge, K. Kanda and T.Minami, Appl. Phys. Lett. 48 (1986) 1739.

[6] A. Srinivasan, K. Ramesh, K.V. Madhusoodana, E.S.R. Gopal. Phil. Mag. Lett. 65 (1992) 249.

[7] L.A. Wahab. Materials Chemistry and Physics 80 (2003) 401-404.

[8] De Michelis f., Kaidakis G., Tagliferro A . and Tresso E., Appl., Optics 9 (1987) 1737.

[9] A.S.Abd Rabo, Kh.M.El-Mokhtar and K.A. Sharaf Al-Azhar Bulletin of Science, Proceedings of the 4th Int. Sci. Conf. 27-29 March 2001, pp. 513-524.

[10] M. Kastner, Phys. Rev. Lett. 28 (1972) 355.

[11] I. Inagawa, R. Iizuka. T. Yamagisni and R. Yokota. J. Non-Cryst. Solids 95 & 96 (1987) 801.